PCCP

Cite this: *Phys. Chem. Chem. Phys.*, 2012, **14**, 13325–13331

www.rsc.org/pccp

PAPER

Theory of pulsed reaction yield detected magnetic resonance

Egor A. Nasibulov,[ab] Leonid V. Kulik,[c] Robert Kaptein[bd] and Konstantin L. Ivanov*[ab]

Received 4th May 2012, Accepted 30th July 2012
DOI: 10.1039/c2cp42117h

We propose pulse sequences for Reaction Yield Detected Magnetic Resonance (RYDMR), which are based on refocusing the zero-quantum coherences in radical pairs by non-selective microwave pulses and using the population of a radical pair singlet spin state as an observable. The new experiments are analogues of existing EPR experiments such as the primary echo, Carr–Purcell, ESEEM, stimulated echo and Mims ENDOR. All pulse sequences are supported by analytical results and numerical calculations. The pulse sequences can be used for more efficient and highly detailed characterization of intermediates of chemical reactions and charge carriers in organic semiconductors.

Introduction

Spin-dependent processes occur frequently in physics and chemistry. In particular, paramagnetic defect states in organic semiconductors can be involved in spin-dependent recombination or transport processes. Due to the presence of spin degrees of freedom one can affect the performance of organic semiconductor devices by applying magnetic fields, which can change the spin state of charge carriers and influence the current. Most notably, the presence of spin degrees of freedom affects the performance of photo-voltaic cells[1–6] and leads to organic magneto-resistance phenomena.[7–9] Many chemical reactions also sense external magnetic fields[10] as they involve pairs of free radicals, whose recombination is typically spin-selective and proceeds preferentially from the singlet state of a radical pair (RP). An important example of spin-dependent chemical reactions is given by light-induced charge separation in photosynthesis.[11–13] There is also evidence that chemical reactions involving transient RPs could be responsible for animal navigation in the earth magnetic field.[14,15]

The traditional way of detecting radical pairs is based on direct observation of their EPR signals. However, this method usually has a low sensitivity. For this reason Reaction Yield Detected Magnetic Resonance (RYDMR) techniques have been developed.[16–30] They enable detection of magnetic resonance spectra indirectly by choosing a different observable, which can be optical absorption or luminescence of the product of RP recombination (optically detected EPR, or OD EPR) or photo-current (electrically detected magnetic resonance, or EDMR).

The aim of the present work is developing pulse sequences and the theoretical framework for pulsed RYDMR and EDMR in order to fully exploit the potential of these methods. Pulsed methods of magnetic resonance are always by far more informative and enable precise spectroscopic characterization of the objects under study. Although the idea of pulsed RYDMR is the same as that of pulsed EPR the problem under consideration is more complicated and pulse sequences for RYDMR cannot be taken from pulsed EPR without modifications. This is because there are two different types of observables: while in EPR spin magnetization is detected, in RYDMR the rate of formation of the reaction product is measured, which is usually proportional to the population of the reactive spin state of a RP. When this state is the singlet state the difference between the two observables is particularly pronounced: once the RP is in the singlet state the reaction rate and, consequently, the RYDMR signal are maximal, whereas all spin magnetization components are equal to zero. For this reason the RYDMR case should be treated separately. In cases where semi-selective pulses are used one can apply standard EPR sequences and add an extra $\pi/2$-pulse in order to convert the spin magnetization echo into a RYDMR echo. This method was originally proposed for triplet-state optically detected magnetic resonance.[31,32] Such pulse sequences were used in EDMR[33,34] and pronounced echo-type signals have been observed. Using the same concept it was possible to obtain more specific information about the systems under study and to observe the echo modulation[35] and pulsed Electron-Nuclear Double Resonance (ENDOR) signals.[36] However, this recipe may not apply when non-selective pulses are used that flip magnetization of both radicals simultaneously. For such a case only a few basic ideas have been proposed.[37,38] It is worth noting that in NMR and EPR spectroscopy the difference

[a] *International Tomography Center SB RAS, Institutskaya 3a, Novosibirsk 630090, Russia. E-mail: ivanov@tomo.nsc.ru; Fax: +7 383 333 1399; Tel: +7 383 333 3861*
[b] *Novosibirsk State University, Pirogova 2, Novosibirsk 630090, Russia*
[c] *Institute of Chemical Kinetics and Combustion SB RAS, Institutskaya 3, Novosibirsk 630090, Russia*
[d] *Bijvoet Center, University of Utrecht, Padualaan 8, NL–3584 CH Utrecht, The Netherlands*

between selective and non-selective pulses is substantial[39] and different pulse sequences should be used depending on the type of excitation. Here we suggest and describe theoretically the main pulse sequences for RYDMR, namely, the primary echo, stimulated echo, Electron Spin Echo Envelope Modulation (ESEEM) and ENDOR sequences. We will restrict ourselves to non-selective μw-pulses that affect both electron spins in the RP.

Theory

It will be assumed that the RP is initially formed in the singlet electronic state and also recombines from the singlet state. These limitations are not essential and are made for the sake of simplicity and clarity; our treatment can be easily extended to the arbitrary initial state and the recombination channel of the RP. Both in liquids and in solids RP recombination is spin-selective.[3,6,9,40–43] We will consider RPs in the solid state, where the distance between the radicals and their orientations is fixed and all the magnetic interactions are constant. In solids it is common that the free induction decay is so fast that observing a spin echo is the only way of detecting the EPR spectra. In most cases we will calculate the spin evolution of a RP in approximations of (i) short non-selective μw-pulses and (ii) neglecting relaxation and chemical reaction. Thus, the effect of each pulse is described by the evolution operator $\hat{R}_\varphi = \exp(-i\varphi\hat{S}_x)$ with φ being the flip angle of the pulse and $\hat{S}_x = \hat{S}_{1x} + \hat{S}_{2x}$ is the x-projection of the spin operator of two electronic spins; μw-pulses are in resonance with the electronic spin transitions of the RP and their bandwidth is sufficient for covering the entire EPR spectrum of the RP. Although providing a sufficiently large B_1-field of the μw-pulses is often a problem in EPR spectroscopy there are situations where it is feasible to use non-selective excitation in EPR of RPs. This is the case, for instance, in EPR studies of photosynthetic reaction centers where the so-called out-of-phase echoes were observed,[12,13,44] which is possible only when non-selective pulses are used. In many organic semiconductor systems, which are studied by EDMR, the width of the EPR spectra of RPs is even smaller.[40] Thus, the assumption of non-selective μw-excitation is realistic for these systems. Neglecting relaxation and chemical reaction is done for simplicity, since it allows one to obtain analytical results and understand how the echoes are formed. Although the chemical reaction is a prerequisite for observing the RP singlet state population, under certain conditions one can omit it when calculating the RP spin evolution. This is the case when the reaction rate is much slower than the spin dynamics but large enough to provide an observable RYDMR signal. A more detailed explanation of the role of chemical reaction will be given below.

Only the case of high external field B_0 parallel to the z-axis will be studied; hyperfine coupling (HFC) of the first electron with one magnetic spin 1/2 nucleus in the RP will be considered. Between pulses the spin evolution can then be described by means of the Hamiltonian $\hat{H}$, which has the form:

$$\hat{H} = \omega_1 S_{1z} + \omega_2 S_{2z} + J S_{1z} S_{2z} + A S_{1z} I_z + B S_{1z} I_x + \omega_1 I_z \quad (1)$$

Here, $\hat{S}_{1z}$ and $\hat{S}_{2z}$ are the operators of z-projection of the electron spins; $\hat{I}_z$ and $\hat{I}_x$ are the operators of z- and x-projections of the nuclear spin, respectively; ω_1 and ω_2 are the electronic Zeeman interactions with the external field; $J = J_0 + D(1 - 3\cos^2\theta)/2$ is the electron spin–spin interaction constant including contributions from exchange, J_0, and dipolar coupling, D, of the electrons with θ being the angle between the vector connecting the electron spins and the external field; A and B are the secular and pseudo-secular parts of the HFC tensor, respectively; ω_I is the nuclear Zeeman interaction. In solids the EPR lines are inhomogeneously broadened so that there is a distribution of ω_1 and ω_2 coming from anisotropic g-tensors of radicals and their random orientations in the solid. We assume that these distributions are Gaussian and have widths of σ_1 and σ_2. In calculations we perform averaging over all possible values of ω_1 and ω_2. Inhomogeneous broadening of EPR lines caused by HFC anisotropy will be neglected here. In eqn (1) we have omitted all other terms in the electron spin–spin interaction and HFC in accordance with the high-field approximation: $\omega_1,\omega_2 \gg A,B$ and $|\omega_1 - \omega_2| \gg |J|$. We will assume that the RPs are formed instantaneously, for instance, with a short laser flash. The initial density matrix of the spin system at $t = 0$ is as follows:

$$\rho_0 = \rho_S \otimes \rho_I \quad (2)$$

where $\rho_S = |S\rangle\langle S|$ is the density matrix of the singlet state of the two electrons and ρ_I is the equilibrium density matrix of the nucleus, which is proportional to the unity matrix $\hat{e}$: $\rho_I = \frac{1}{2}\hat{e}$

Spin evolution of the RP is calculated as follows. The density matrix of the spin system obeys the Liouville–von Neumann equation:

$$\frac{d\rho(t)}{dt} = -i[\hat{H}, \rho] - \frac{K_S}{2}\{\hat{P}_S, \rho\} \quad (3)$$

Here $[\ldots]$ and $\{\ldots\}$ denote the commutator and anti-commutator, respectively; K_S is the rate of the singlet-state recombination; $\hat{P}_S$ is the operator of projecting on the RP singlet spin state. An anti-commutator form of the reaction term in eqn (3) is a proper way of modeling spin-selective chemical reactions.[45–48] The rate of the product formation, $F(t)$, is given by the following quantity:

$$F(t) = K_S \rho_{SS}(t) \quad (4)$$

In RYDMR experiments this rate is used as an observable; $F(t)$ is monitored by measuring optical absorption, fluorescence or photo-current. For instance, in the case of fluorescence detection the signal observed at time t is given by[20]

$$\frac{1}{\tau_{fl}}\int_0^t \exp(-(t-\tau)/\tau_{fl})F(\tau)d\tau \quad (5)$$

which is reduced to $F(t)$ at short fluorescence time, τ_{fl}.[20] Hereafter we will calculate the rate, $F(t)$, and the RP singlet-state population, $\rho_{SS}(t)$. When the optical absorption $A(t)$ of the reaction products is used for detection, studying the RP spin dynamics is more problematic. This is because not the quantity of interest, $F(t)$, is measured but its time integral, $A(t)$. For this reason our treatment is appropriate for experiments where the product fluorescence is used as an observable.

Each period of free evolution of duration τ modifies the density matrix in the following way:

$$\rho(t + \tau) = \exp(-(i\hat{H} + K_S\hat{P}_S/2)\tau)\rho(t)\exp((i\hat{H} - K_S\hat{P}_S/2)\tau) \quad (6)$$

In turn, the action of a pulse with duration τ_p and flip angle φ changes the density matrix as follows:

$$\rho(t + \tau_p) = \hat{R}(\varphi)\rho(t)\hat{R}^{-1}(\varphi) = \exp(-i\varphi\hat{S}_x)\rho(t)\exp(i\varphi\hat{S}_x) \quad (7)$$

Then we calculate the singlet state population as $\rho_{SS}(t) = \langle S|\rho(t)|S\rangle$ and average this quantity over all realizations of ω_1 and ω_2. In the numerical calculations averaging is done by summing the calculation results for different ω_1 and ω_2, whereas in the analytical calculations we set all terms containing $\exp(\pm i(\omega_1 - \omega_2)\tau)$ equal to zero. For all pulse sequences we will calculate the echo height analytically, while all the kinetic traces will be computed numerically.

Results and discussion

Let us now discuss how the echo is formed when the singlet state population is chosen as an observable. First of all, we will describe dephasing processes existing in RPs. As in standard EPR one can create single-quantum coherences by μw-pulses and refocus them; however, the RPs provide an additional option. In high magnetic field the singlet state is not an eigen-state of the Hamiltonian (1) and therefore the RP starting from the $|S\rangle$ state undergoes coherent spin evolution. Its population oscillates between $|S\rangle$ and $|T_0\rangle$ states with the frequency of oscillation being equal to $|\omega_1 - \omega_2|$ in the absence of HFC, *i.e.*, $\rho_{SS}(t) = \cos^2\frac{(\omega_1-\omega_2)t}{2}$ and $\rho_{T_0T_0}(t) = \sin^2\frac{(\omega_1-\omega_2)t}{2}$. When there is a distribution of ω_1 and ω_2 the oscillations become damped and the populations are evenly distributed between the $|S\rangle$ and $|T_0\rangle$ states: ρ_{SS} goes from 1 to 1/2 on the timescale of $(1/\sigma_1 + 1/\sigma_2)$. Thus, the zero-quantum coherence (ZQC) between the eigen-states $|\alpha\beta\rangle$ and $|\beta\alpha\rangle$ is dephased. As this process is not stochastic but coherent, the ZQC can be refocused by μw-pulses. In contrast to the EPR case, in RYDMR a single π-pulse applied at $t = \tau$ can completely refocus the singlet state population, *i.e.*, $\rho_{SS} = 1$, at $t = 2\tau$ (ref. 37) and an echo-type signal should be observed. This is because the laser pulse that creates the RPs plays the role of the first pulse in the primary echo sequence as it produces coherences in the system.

We will employ the same idea of refocusing ZQC to obtain more complicated echo sequences. Before going to the calculations it is important to formulate the condition for observing an echo in RYDMR. It is obvious that only having a non-zero value of ρ_{SS} is not sufficient for refocusing, *i.e.*, for observing an echo. This is because the population can be rapidly and evenly distributed between $|S\rangle$ and $|T_0\rangle$ states due to the condition $(\omega_1 - \omega_2) \neq 0$ and part of the population can also go to the $|T_+\rangle$ and $|T_-\rangle$ states. Since refocusing of ZQC means that ρ_{SS} and $\rho_{T_0T_0}$ differ, the criterion of observing an echo at time instant τ_{echo} is as follows: $\rho_{SS}(\tau_{echo}) \neq \rho_{T_0T_0}(\tau_{echo})$. Between the two subsequent pulses ρ_{SS} is equal to a constant value $\rho_{av} = \frac{\rho_{SS}(\tau_{echo})+\rho_{T_0T_0}(\tau_{echo})}{2}$, while at $t = \tau_{echo}$ an echo of the height $\frac{\rho_{SS}(\tau_{echo})-\rho_{T_0T_0}(\tau_{echo})}{2}$ appears as a peak in $\rho_{SS}(t)$ with a width of $(1/\sigma_1 + 1/\sigma_2)$.

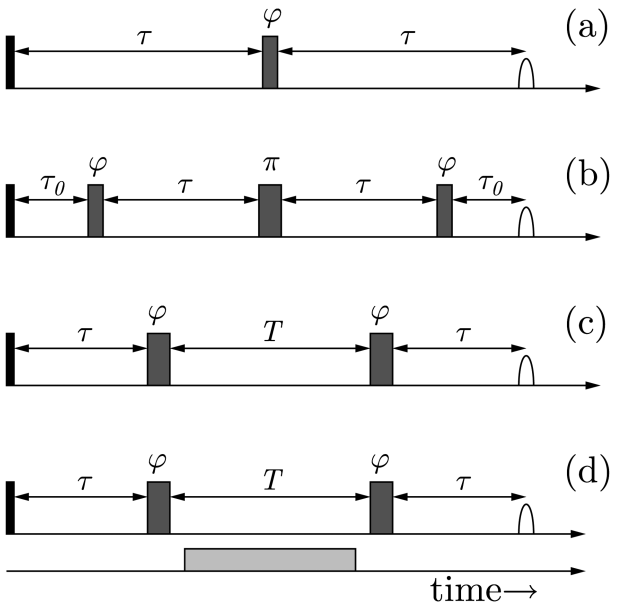

Fig. 1 Pulse sequences for RYDMR: primary echo (a), ESEEM (b), stimulated echo (c) and ENDOR (d). Laser pulses are shown in black, μw-pulses are shown in dark grey, rf-pulse is shown in light grey, echo is shown in white; delays and flip angles are indicated.

In order to make clear how refocusing of ZQC manifests itself in the rate, $F(t)$, of the reaction product formation we performed numerical calculations. $F(t)$ was computed by solving eqn (3) for different recombination rates, K_S, and considering the simplest pulse sequence shown in Fig. 1a with a single μw-pulse applied at $\tau = 80$ ns; a flip angle $\varphi = 2\pi/3$ was taken. The $F(t)$ kinetics exhibits exponential decay; however, on top of this decay additional features are seen, which are due to the evolution of ZQC (see Fig. 2). First, on the timescale of $(1/\sigma_1 + 1/\sigma_2)$ there are fast oscillations, which are due to the dephasing of ZQC. Second, after applying a μw-pulse at $t = \tau$ the singlet state population is not changed immediately

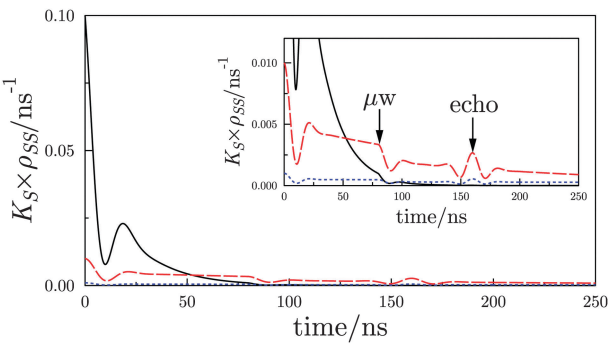

Fig. 2 Rate of product formation, $F(t) = K_S\rho_{SS}(t)$ as a function of time calculated for the pulse sequence from Fig. 1a for different K_S: 0.1 ns^{-1} (solid line), 0.01 ns^{-1} (dashed line), 0.001 ns^{-1} (dotted line). Inset shows the region where the echo is formed; arrows indicate instants of time where the μw-pulse is applied and the echo is formed. Calculation parameters are: $\tau = 80$ ns, $\varphi = 2\pi/3$, $(\omega_1 - \omega_2) = 1.5$ mT, $\sigma_1 = 0.5$ mT, $\sigma_2 = 0$, $J = 0$, $A = B = 0$.

(because the non-selective excitation does not change the total electron spin of the RP) but an additional ZQC is formed, since at $\varphi \neq n\pi$ $\rho_{T_0T_0}$ is reduced (population partly goes to the $|T_+\rangle$ and $|T_-\rangle$ states) and ZQC is proportional to $(\rho_{SS} - \rho_{T_0T_0})$. Subsequently, this ZQC is rapidly dephased. Finally, at $t = 2\tau$ there is an echo seen, which is coming from a partial refocusing of the initial ZQC by the pulse. Thus, when $F(t)$ is an experimental observable one can detect echo-like signals coming from refocusing ZQC by short μw-pulses.

In this context it is important to discuss the optimal K_S value. A high K_S results in high product yield, but it also leads to rapid RP decay and makes the spin echoes undetectable. This situation is demonstrated by solid line in Fig. 2. Having a slow recombination rate (case shown by dotted line in Fig. 2) is advantageous as far as a possibility of refocusing spin coherences is concerned; however, it also results in low rates of the product formation and lower RYDMR signals. Thus, for detecting the echo signals is it optimal to have intermediate K_S values (dashed line in Fig. 2). Hereafter we will assume that K_S is such that (i) $F(t)$ is detectable and (ii) recombination is considerably slower than the spin evolution given by the Hamiltonian $\hat{H}$ from eqn (1). These assumptions are realistic, for instance, in EDMR where echo-type signals have been observed.[33,34] Under such conditions it is also possible to affect the RP lifetimes by applying short μw-pulses.[43,49] Once the reactivity is low it can also be treated as a perturbation, which almost does not change the spin evolution but nevertheless transfers the RP singlet-state population, $\rho_{SS}(t)$, into the detectable quantity $F(t)$. In this situation it is sufficient to calculate $\rho_{SS}(t)$ neglecting the effect of the reaction on the spin dynamics.[50] Hereafter, we will use this approximation for the sake of simplicity and clarity.

Let us now describe theoretically the RYDMR analogues of the main EPR pulse sequences. Following ref. 37 we will first verify whether the primary echo can be obtained with a single μw-pulse when the RPs are instantaneously produced at $t = 0$. We will consider the simplest pulse sequence shown in Fig. 1a comprising one laser pulse and one μw-pulse with arbitrary flip angle φ separated by a time interval τ. When the HFC terms are neglected ($A = B = 0$) the following results for ρ_{SS} and $\rho_{T_0T_0}$ at $t = 2\tau$ can be obtained:

$$\rho_{SS}(2\tau) = \frac{9 - 4\cos\varphi + 3\cos 2\varphi}{16}$$
$$\rho_{T_0T_0}(2\tau) = \frac{3 + 4\cos\varphi + \cos 2\varphi}{16} \quad (8)$$

Since

$$\rho_{SS}(2\tau) - \rho_{T_0T_0}(2\tau) = \sin^4\frac{\varphi}{2} \neq 0 \quad (9)$$

there is an echo-type signal at $t = 2\tau$. The echo amplitude is maximal at $\varphi = (2n + 1)\pi$, $n \in Z$ because a π-pulse completely reverts the evolution of the ZQC, but a primary echo can be observed at any $\varphi \neq 2n\pi$, $n \in Z$. It is important to note that

$$\rho_{av}(2\tau) = \frac{\rho_{SS}(2\tau) + \rho_{T_0T_0}(2\tau)}{2} = \frac{\cos^2\varphi + 1}{4} \quad (10)$$

is less than 1/2 when $\varphi \neq n\pi$, $n \in Z$. This is because at arbitrary φ angle some part of the RPs is converted by the μw-pulse to the $|T_+\rangle$ and $|T_-\rangle$ states and never comes back into the S–T_0 manifold.

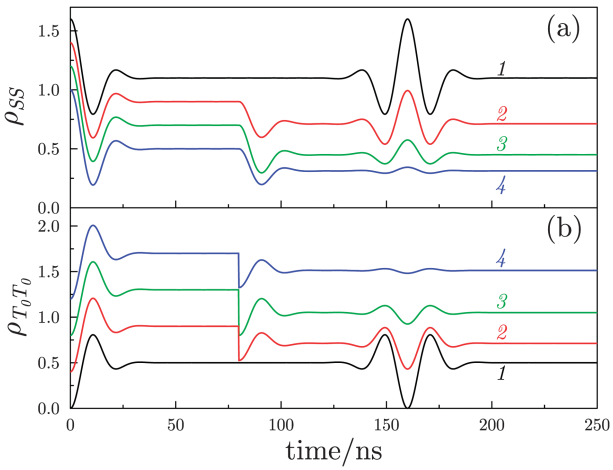

Fig. 3 Time evolution of $\rho_{SS}(t)$ (a) and $\rho_{T_0T_0}(t)$ (b) for the primary echo sequence calculated for flip angles π (1), $2\pi/3$ (2), $\pi/2$ (3) and $\pi/3$ (4). Curves for different φ are shifted along the vertical; the numbers on the vertical scale are related to curves 4 (a) and 1 (b); calculation parameters: $(\omega_1 - \omega_2) = 1.5$ mT, $\sigma_1 = 0.5$ mT, $\sigma_2 = 0$, $J = 0$, $A = B = 0$, $\tau = 80$ ns.

The time evolution of $\rho_{SS}(t)$ and $\rho_{T_0T_0}(t)$ is shown in Fig. 3 for flip angles of π, $2\pi/3$, $\pi/2$ and $\pi/3$. In all cases $\rho_{SS}(t)$ rapidly decays from 1 to 1/2 after the laser pulse. Applying the π-pulse results in complete refocusing at $t = 2\tau$, which is seen as a peak in the $\rho_{SS}(t)$ dependence (Fig. 3a). After applying a μw-pulse with smaller φ, ρ_{SS} and $\rho_{T_0T_0}$ decrease because part of the RPs goes to the $|T_\pm\rangle$ states. However, ρ_{SS} and $\rho_{T_0T_0}$ behave differently: while $\rho_{T_0T_0}$ decreases abruptly under the action of the pulse, ρ_{SS} can only change later due to the subsequent evolution of ZQC created by the pulse. The peak at $t = 2\tau$ is still seen although its height is reduced. Each peak in the $\rho_{SS}(t)$ dependence (Fig. 3a) is accompanied by a dip in $\rho_{T_0T_0}(t)$ (Fig. 3b).

Refocusing of the ZQC can be used in more complicated pulse sequences. For instance, one can implement an analogue of the Carr–Purcell sequence by introducing after a delay τ after the laser pulse a train of π-pulses separated by equal intervals of 2τ. In this case there will be echoes seen at times $t_n = 2n\tau$ in the $\rho_{SS}(t)$ kinetics trace and their decay can be used to study spin relaxation in the RP.

Now let us take $A,B \neq 0$ and discuss the effects of the ESEEM. The most obvious source of modulation is provided by anisotropic HFC, which is a common ESEEM mechanism in X-band EPR.[51] Due to the presence of the B-term in eqn (1) the $|\alpha\rangle$ and $|\beta\rangle$ states of the nucleus are no longer the eigenstates of the spin system but become mixed. We have calculated the primary echo (sequence from Fig. 1a) amplitude taking the full Hamiltonian (1) and assuming $\varphi = \pi$ (the case of arbitrary φ will not be discussed here). The calculation gives the following result:

$$\rho_{SS}(2\tau) = 1 - \frac{{\omega_I}^2 B^2}{4{\omega_\alpha}^2{\omega_\beta}^2}\sin^2\left(\frac{\omega_\alpha\tau}{2}\right)\sin^2\left(\frac{\omega_\beta\tau}{2}\right) \quad (11)$$

Here $\omega_{\alpha,\beta}$ are

$$\omega_{\alpha,\beta} = \frac{1}{2}\sqrt{(A \pm 2\omega_I)^2 + B^2} \quad (12)$$

ESEEM of this type allows one to obtain information about the HFC tensor.

It is also of interest to obtain the ESEEM caused by the electron spin–spin interaction, J. In general, studies of the echo modulation can provide information about the distance between the radicals of the RP, which is now seen as one of the most important applications of EPR.[52,53] For obtaining such type of ESEEM in RYDMR it is necessary to modify the pulse sequence. We have found that two μw-pulses are not sufficient to obtain modulation caused by J, but at least three pulses are necessary. An appropriate sequence for ESEEM can be found using the fact[12,13] that the sequence laser–(delay τ_0)–(π/4-pulse)–(delay τ)–(π-pulse) allows one to observe the modulated out-of-phase echo signal in EPR of RPs. The same pulse sequence can be used in RYDMR with a slight modification: a third μw-pulse can be added to convert the EPR echo into the RYDMR echo. Thus, we consider the pulse sequence shown in Fig. 1b. For this sequence we have obtained the following expressions for the state populations at $t = 2\tau_0 + 2\tau$:

$$\rho_{SS}(2\tau_0 + 2\tau) = \frac{3\cos^2 2\varphi + 2\cos 2\varphi + 11}{16} + \cos J\tau \frac{3\cos^2 2\varphi + 2\cos 2\varphi - 5}{16} \quad (13)$$

$$\rho_{T_0T_0}(2\tau_0 + 2\tau) = (1 + \cos J\tau)\frac{(1 - \cos 2\varphi)^2}{16}$$

The echo is given by the following expression:

$$\rho_{SS}(2\tau + T) - \rho_{T_0T_0}(2\tau + T) = (1 + \cos 2\varphi)^2 \frac{1 + \cos J\tau}{8} + \frac{1 - \cos J\tau}{2} \quad (14)$$

Since $\rho_{SS}(2\tau_0 + 2\tau) \neq \rho_{T_0T_0}(2\tau_0 + 2\tau)$ there is an echo formed, which contains a modulation term proportional to $\cos(J\tau)$. It is important that the echo at $t = (2\tau_0 + 2\tau)$ does not depend on the time interval τ_0, which can therefore be taken arbitrarily and there is no need to set τ_0 separately for optimizing the echo signal.

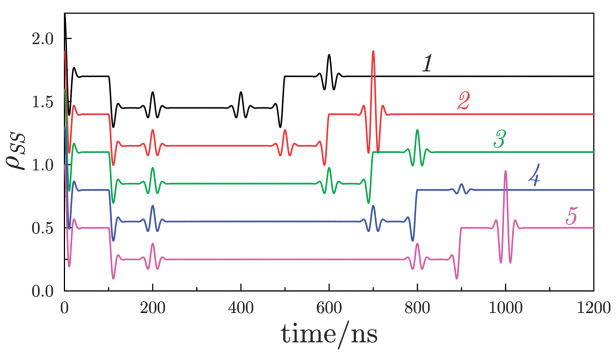

Fig. 4 Time evolution of $\rho_{SS}(t)$ for the ESEEM sequence calculated for different delays τ: 200 ns (1), 250 ns (2), 300 ns (3), 350 ns (4), 400 ns (5). Curves are shifted along the vertical; the numbers on the vertical scale are related to curve 5; calculation parameters: $\varphi = \pi/2$; $(\omega_1 - \omega_2) = 1.5$ mT, $\sigma_1 = 0.5$ mT, $\sigma_2 = 0$, $J = 0.5$ mT, $A = B = 0$, $\tau_0 = 100$ ns.

Kinetic traces for ρ_{SS} are shown in Fig. 4. There is an echo clearly seen at $t = 2\tau_0 + 2\tau$. In the kinetics there are more echoes because the laser pulse in combination with any of the three μw-pulses gives three primary echoes; there are also echoes coming from laser and two μw-pulses. In addition, the situation is complicated by the stepwise variation of the ρ_{av} level caused by the μw-pulses because they induce transitions between the S–T_0 and T_+–T_- manifolds. Here we are interested only in the ESEEM of the echo at $t = 2\tau_0 + 2\tau$ that changes with τ, *i.e.* contains the desired modulation. When the spin–spin interaction is caused by dipolar coupling, D, and there is a random set of all possible orientations, θ, the inverse Fourier transform of the modulated part of the echo will give the in-phase Pake doublet. The distance between the components of the doublet gives the D value, which is unambiguously related to the distance between the radical centers in the RP.[12,52,53]

Finally, let us find an analogue of the stimulated echo sequence, which also allows one to obtain an ENDOR sequence after a slight modification. To obtain the stimulated echo we will follow ideas from conventional NMR and EPR. The refocusing pulse in the primary echo signal can be cut into two halves separated by a time interval T, which gives the stimulated echo at $t = 2\tau + T$ coming from all the pulses of the sequence. Thus, we propose to use the pulse sequence shown in Fig. 1c. The values of the state populations of interest at $t = 2\tau + T$ are as follows:

$$\rho_{SS}(2\tau + T) = \frac{1}{32}(\cos 2\varphi + 3)^2 + \frac{1}{4}\sin^4\varphi, \qquad \rho_{T_0T_0}(2\tau + T) = \frac{1}{32}(\cos 2\varphi + 3)^2 \quad (15)$$

The echo is described by the formula:

$$\rho_{SS}(2\tau + T) - \rho_{T_0T_0}(2\tau + T) = \frac{1}{4}\sin^4\varphi \quad (16)$$

which is similar to eqn (9): only the coefficient is different and $\varphi/2$ is replaced by φ because two μw-pulses are used and the total flip angle is thus doubled. The optimal flip angle for the largest value of the echo is thus $\varphi = \pi/2$. The calculated

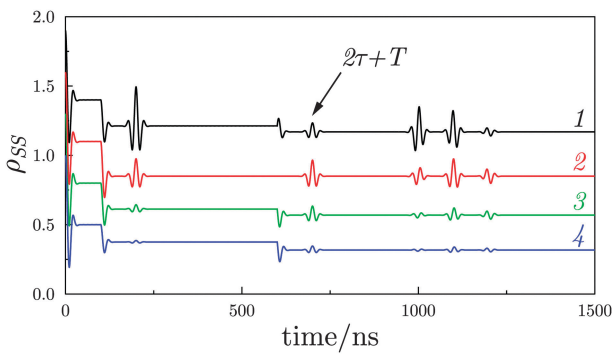

Fig. 5 Time evolution of $\rho_{SS}(t)$ for the stimulated echo sequence calculated for different φ: $2\pi/3$ (1), $\pi/2$ (2), $\pi/3$ (3), $\pi/4$ (4); the stimulated echo is indicated by arrow. Curves are shifted along the vertical axis; the numbers on the vertical scale are related to curve 4; calculation parameters: $(\omega_1 - \omega_2) = 1.5$ mT, $\sigma_1 = 0.5$ mT, $\sigma_2 = 0$, $J = 0$, $A = B = 0$, $\tau = 100$ ns, $T = 500$ ns.

kinetic traces of ρ_{SS} for the stimulated echo sequence are shown in Fig. 5. One can see several echoes (as in the EPR case). However, only one of them is caused by the laser pulse and both μw-pulses: this is an echo at $t = 2\tau + T$ that is a direct analogue of the stimulated echo.

To justify the analogy with the conventional stimulated echo in EPR it is also necessary to show that the echo at $t = 2\tau + T$ can be formed despite the relaxation losses of coherences between the μw-pulses. To demonstrate this we made an analytical calculation of $\rho_{SS}(2\tau + T)$ and $\rho_{T_0T_0}(2\tau + T)$ taking spin relaxation into account. In the calculation we assumed that both electron spins relax with the same times, T_1 and T_2, of the longitudinal and transverse relaxation, respectively, additionally, $T_1 \gg T_2$ and $T \gg T_2$. In this situation all coherences in the spin system rapidly disappear after the first μw-pulse, while the state populations relax to their equilibrium values between the μw-pulses. The second μw-pulse converts the partially relaxed state populations into ZQC and refocusing takes place. In this model we obtained the following results for the state populations of interest at $t = 2\tau + T$:

$$\begin{aligned}\rho_{SS}(2\tau+T) &= \frac{1}{4}+\frac{1}{12}\exp\left(-\frac{2T}{T_1}\right)\\ &\quad+\frac{3}{32}\exp\left(-\frac{2T}{T_1}\right)\left(\cos 2\varphi+\frac{1}{3}\right)^2,\\ \rho_{T_0T_0}(2\tau+T) &= \frac{1}{4}\left(1-\exp\left(-\frac{2T}{T_1}\right)\right)\\ &\quad+\frac{1}{32}\exp\left(-\frac{2T}{T_1}\right)(\cos 2\varphi+3)^2\end{aligned} \quad (17)$$

As compared to eqn (16) the echo is multiplied by a factor of $\exp(-2T/T_1)$:

$$\rho_{SS}(2\tau+T)-\rho_{T_0T_0}(2\tau+T)=\frac{1}{4}\exp\left(-\frac{2T}{T_1}\right)\sin^4\varphi \quad (18)$$

Thus, the echo does not disappear despite the fast transverse relaxation and is only modified due to T_1-relaxation.

An analogue of the Mims ENDOR sequence[51] follows naturally from the stimulated echo sequence. Reaction yield detected ENDOR can be of importance due to the extraordinary spectroscopic capabilities of the ENDOR methods.[51,54] The idea of ENDOR in our case is as follows. In the stimulated echo sequence the delay T can be taken so long that it is possible to apply an rf-pulse that can flip the nuclear spins. As a consequence, during the dephasing period ($0 < t < \tau$) and the refocusing period ($\tau + T < t < 2\tau + T$) the electronic spin experiences different HFC and the stimulated echo becomes modulated. By studying this modulation one can obtain the value of the HFC constant, A.

The corresponding pulse sequence is shown in Fig. 1d. Here the μw-pulses are the same as in the stimulated echo sequence but in addition a long selective rf-pulse is applied between the μw-pulses. It flips the nuclear spins by an angle π. As a consequence, the frequencies of the electron spin differ by $\varpi = A$ (B is taken to be zero) during dephasing and refocusing giving the following ρ_{SS} and $\rho_{T_0T_0}$ values at $t = 2\tau + T$:

$$\begin{aligned}\rho_{SS}(2\tau+T) &= \frac{1}{32}\left((3+\cos 2\varphi)^2+8\cos^2\frac{\varpi\tau}{2}\sin^4\varphi\right);\\ \rho_{T_0T_0}(2\tau+T) &= \frac{1}{32}\left((3+\cos 2\varphi)^2+8\sin^2\frac{\varpi\tau}{2}\sin^4\varphi\right).\end{aligned} \quad (19)$$

Thus, as in Mims ENDOR there is a modulation: the stimulated echo amplitude depends not only on φ but also on $(\varpi\tau)$:

$$\rho_{SS}(2\tau_1+\tau_2)-\rho_{T_0T_0}(2\tau_1+\tau_2)=\frac{1}{4}\cos\varpi\tau\sin^4\varphi \quad (20)$$

By varying the delay τ and scanning the rf-frequency one can precisely determine the HFC properties from the echo signal.

Conclusions

We have developed the theory of pulsed RYDMR and suggest analogues of the main EPR pulse sequences in the case of non-selective μw-pulses. We have used refocusing of the ZQC in the RP and formulated a criterion for observing spin echoes in RYDMR where not the spin magnetization but the singlet state population is used as an observable. The primary echo sequence has been studied, which can be extended to an analogue of the Carr–Purcell sequence with multiple echoes coming from subsequent pulses. We have suggested an ESEEM pulse sequence for observing modulations caused by the electronic spin–spin interactions that can be used to probe the distance between the radicals in the RP. Finally, an analogue of the stimulated echo sequence and the Mims ENDOR sequence have been proposed.

The theoretical results can be used to extend the scope of RYDMR spectroscopy and fully exploit its potential. In combination with the high sensitivity of RYDMR, techniques using pulsed methods can provide new attractive options for more detailed study of structure, dynamics and reactivity of the short-lived RPs and properties of paramagnetic charge carriers in organic semiconductors.

Acknowledgements

Financial support from RFBR (projects No. 11-03-00356, 11-03-00296, 12-03-00238), Program of the Presidium of RAS (grant No. 23/24.48) and the Program P-220 of the Russian Government (grant No. 11.G34.31.0045) is gratefully acknowledged. We are thankful to Prof. H.-M. Vieth, Prof. R. Bittl and Dr J. Behrends (Free University of Berlin) for stimulating discussions.

Notes and references

1 D. R. McCamey, K. J. van Schooten, W. J. Baker, S.-Y. Lee, S.-Y. Paik, J. M. Lupton and C. Boehme, *Phys. Rev. Lett.*, 2010, **104**, 017601.
2 D. R. McCamey, H. A. Seipel, S.-Y. Paik, M. J. Walter, N. J. Borys, J. M. Lupton and C. Boehme, *Nat. Mater.*, 2008, **7**, 723–728.
3 J. M. Lupton, D. R. McCamey and C. Boehme, *ChemPhysChem*, 2010, **11**, 3040–3058.
4 J. Behrends, K. Lips and C. Boehme, *Phys. Rev. B: Condens. Matter Mater. Phys.*, 2009, **80**, 045207.

5 F. Wang, J. Rybicki, K. A. Hutchinson and M. Wohlgenannt, *Phys. Rev. Lett.*, 2011, **83**, 241202.
6 S. P. Kersten, A. J. Schellekens, B. Koopmans and P. A. Bobbert, *Phys. Rev. Lett.*, 2011, **106**, 197402.
7 P. A. Bobbert, W. Wagemans, F. W. A. van Oost, B. Koopmans and M. Wohlgenannt, *Phys. Rev. Lett.*, 2009, **102**, 156604.
8 J. M. Lupton and C. Boehme, *Nat. Mater.*, 2008, **7**, 598.
9 W. Wagemans and B. Koopmans, *Phys. Status Solidi B*, 2011, **248**, 1029–1041.
10 U. E. Steiner and T. Ulrich, *Chem. Rev.*, 1989, **89**, 51.
11 K. Möbius, *Phys. Chem. Chem. Phys.*, 2000, **29**, 129–139.
12 R. Bittl and S. G. Zech, *Biochim. Biophys. Acta*, 2001, 1507.
13 A. J. Hoff, P. Gast, S. A. Dzuba, C. R. Timmel, C. E. Fursman and P. J. Hore, *Spectrochim. Acta, Part A*, 1998, **54**, 2283–2293.
14 C. T. Rodgers and P. J. Hore, *Proc. Natl. Acad. Sci. U. S. A.*, 2009, **106**, 353–360.
15 K. Maeda, C. J. Wedge, J. G. Storey, K. B. Henbest, P. A. Liddell, G. Kodis, D. Gust, P. J. Hore and C. R. Timmel, *Chem. Commun.*, 2011, **47**, 6563–6565.
16 A. Matsuyama, K. Maeda and H. Murai, *J. Phys. Chem. A*, 1999, 103.
17 T. Miura, A. M. Scott and M. R. Wasielewski, *J. Phys. Chem. C*, 2010, **114**, 20370–20379.
18 G. Grampp, M. Justinek and S. Landgraf, *Mol. Phys.*, 2002, **100**, 1063–1070.
19 D. V. Stass, N. N. Lukzen, B. M. Tadjikov, V. M. Grigoryantz and Y. N. Molin, *Chem. Phys. Lett.*, 1995, **243**, 533–539.
20 V. A. Bagryansky, V. I. Borovkov and Y. N. Molin, *Phys. Chem. Chem. Phys.*, 2004, **6**, 924–928.
21 V. N. Verkhovlyuk, D. V. Stass, N. N. Lukzen and Y. N. Molin, *Chem. Phys. Lett.*, 2005, **413**, 71–77.
22 C. T. Rodgers, C. J. Wedge, S. A. Norman, P. Kukura, K. Nelson, N. Baker, K. Maeda, K. B. Henbest, P. J. Hore and C. R. Timmel, *Phys. Chem. Chem. Phys.*, 2009, **11**, 6569–6572.
23 E. V. Gorelik, N. N. Lukzen, R. Z. Sagdeev and H. Murai, *Phys. Chem. Chem. Phys.*, 2003, **5**, 5438–5443.
24 T. Itoh, A. Matsuyama, K. Maeda and H. Murai, *Chem. Phys. Lett.*, 2001, **333**, 242–247.
25 K. Pal, D. R. Kattnig, G. Grampp and S. Landgraf, *Phys. Chem. Chem. Phys.*, 2012, **14**, 3155–3161.
26 O. B. Morozova, K. L. Ivanov, A. S. Kiryutin, R. Z. Sagdeev, T. Köchling, H.-M. Vieth and A. V. Yurkovskaya, *Phys. Chem. Chem. Phys.*, 2011, **13**, 6619–6627.
27 S. N. Batchelor, K. A. McLauchlan and I. A. Shkrob, *Chem. Phys. Lett.*, 1991, **181**, 327–334.
28 S. N. Batchelor, K. A. McLauchlan and I. A. Shkrob, *Mol. Phys.*, 1992, **75**, 531–561.
29 S. N. Batchelor, C. W. M. Kay, K. A. McLauchlan and I. A. Shkrob, *J. Phys. Chem.*, 1993, **97**, 13250–13258.
30 I. A. Shkrob and A. D. Trifunac, *J. Phys. Chem.*, 1996, **100**, 14681–14687.
31 W. G. Breiland, H. C. Brenner and C. B. Harris, *J. Chem. Phys.*, 1975, **62**, 3458–3475.
32 J. Wrachtrup, C. von Borczyskowski, J. Bernard, R. Brown and M. Orrit, *Chem. Phys. Lett.*, 1995, **245**, 262–267.
33 J. M. Lu, F. Hoehne, A. R. Stegner, L. Dreher, M. Stutzmann, M. S. Brandt and H. Huebl, *Phys. Rev. B: Condens. Matter Mater. Phys.*, 2011, **83**, 235201.
34 D. R. McCamey, C. Boehme, G. W. Morley and J. van Tol, *Phys. Rev. B: Condens. Matter Mater. Phys.*, 2012, **85**, 073201.
35 F. Hoehne, J. M. Lu, A. R. Stegner, M. Stutzmann and M. S. Brandt, *Phys. Rev. Lett.*, 2011, **106**, 196101.
36 F. Hoehne, L. Dreher, H. Huebl, M. Stutzmann and M. S. Brandt, *Phys. Rev. Lett.*, 2011, **106**, 187601.
37 K. M. Salikhov and Y. N. Molin, *J. Phys. Chem.*, 1993, **97**, 13259–13266.
38 I. A. Shkrob, *Chem. Phys. Lett.*, 1994, **220**, 347–352.
39 R. R. Ernst, G. Bodenhausen and A. Wokaun, *Principles of Nuclear Magnetic Resonances in One and Two Dimensions*, Clarendon Press, Oxford, 1978.
40 J. Behrends, PhD Thesis, Free University of Berlin, 2009.
41 P. A. Bobbert, T. D. Nguyen, W. Wagemans, F. W. A. van Oost, B. Koopmans and M. Wohlgenannt, *Synth. Met.*, 2010, **160**, 223–229.
42 F. Hoehne, H. Huebl, B. Galler, M. Stutzmann and M. S. Brandt, *Phys. Rev. Lett.*, 2010, **104**, 046402.
43 S. A. Dzuba, I. I. Proskuryakov, R. J. Hulsebosch, M. K. Bosch, P. Gast and A. J. Hoff, *Chem. Phys. Lett.*, 1996, **253**, 361–366.
44 M. C. Thurnauer and J. R. Norris, *Chem. Phys. Lett.*, 1980, **76**, 557–561.
45 R. Haberkorn, *Mol. Phys.*, 1976, **32**, 1491–1493.
46 K. L. Ivanov, M. V. Petrova, N. N. Lukzen and K. Maeda, *J. Phys. Chem. A*, 2010, **114**, 9447–9455.
47 A. I. Shushin, *J. Chem. Phys.*, 2010, **133**, 044505.
48 M. Tiersch, U. E. Steiner, S. Popescu and H. J. Briegel, *J. Phys. Chem. A*, 2012, **116**, 4020–4028.
49 T. Miura and M. R. Wasielewski, *J. Am. Chem. Soc.*, 2011, **133**, 2844–2847.
50 K. Schulten and P. G. Wolynes, *J. Chem. Phys.*, 1978, **68**, 3292–3297.
51 A. Schweiger and G. Jeschke, *Principles of pulse electron paramagnetic resonance*, Oxford University Press, 2001.
52 G. Jeschke, *ChemPhysChem*, 2002, **3**, 927–932.
53 Y. D. Tsvetkov, A. D. Milov and A. G. Maryasov, *Usp. Khim.*, 2008, **77**, 515–550.
54 L. Kulik and W. Lubitz, *Photosynth. Res.*, 2009, **102**, 391–401.